JP Journal of Heat and Mass Transfer
Volume 3, Number 3, 2009, Pages 235-252
Published Online: November 26, 2009
This paper is available online at http://www.pphmj.com

PERISTALTIC FLOW AND HEAT TRANSFER OF A CONDUCTING FLUID IN AN ASYMMETRIC CHANNEL

G. RAMI REDDY, P. V. SATYA NARAYANA[*], S. VENKATARAMANA and S. SREENADH

Department of Mathematics
S. V. University
Tirupati, A. P., India
e-mail: gunapatiramireddy@yahoo.com

[*]Department of Mathematics
VIT University
Vellore, Tamilnadu, India
e-mail: pvsatya8@yahoo.co.in

Abstract

The aim of the present work is to study the MHD peristaltic flow in a two-dimensional asymmetric channel under the assumptions of long wavelength and low Reynolds number in a wave frame of reference with heat transfer. The effects of phase shift and Hartmann number on the pumping characteristics are discussed in detail through graphs.

1. Introduction

The magnetohydrodynamic (MHD) flow of a fluid in a channel with elastic rhythmically contracting walls (peristaltic transport) is of interest in connection with certain flow problems of the movement of conductive physiological fluids and with the need for theoretical research on the operation of a peristaltic MHD compressor, also the principle of magnetic field may be used in clinical application (magnetic resonance imaging MRI). Agrawal and Anwaruddin [1] studied the effect of

Keywords and phrases: peristaltic flow, MHD, heat transfer.

Received July 11, 2009

magnetic field on the peristaltic flow of blood using long wavelength approximation method and observed for the flow of blood in arteries with arterial stenosis or arteriosclerosis, that the influence of magnetic field may be utilized as blood pump in carrying out cardiac operations. Li et al. [2] have used an impulsive magnetic field in the combined therapy of patients with stone fragments in the upper urinary tract. It was found that the Impulsive Magnetic Field (IMF) activates the impulsive activity of the ureteral smooth muscles in 100% of cases. Nonlinear peristaltic transport of MHD flow through a porous medium was studied by Mekheimer and Al-Arabi [4]. Mekheimer [3] studied the peristaltic transport of blood under effect of a magnetic field in non-uniform channels. Some of the physiological systems in human body cannot be modeled by a symmetrical channel, especially the sagittal cross section of the uterus. Recently, Mishra and Rao [5] developed the flow in an asymmetric channel generated by peristaltic waves propagating on the walls. Mishra and Rao [5] obtained a perturbation solution for the problem of peristaltic flow of a viscous Newtonian fluid in an asymmetric channel. Most of these studies are without heat transfer. In general, heat transfer will play vital role on peristalsis. Peristaltic transport of a heat conducting fluid subject to Newton's cooling law at the boundary was investigated by Tang and Shen [7]. Tang and Shen [8] studied asymptotic solutions for the peristaltic flow of a heat conducting fluid. Motivated by these, we modeled the peristaltic transport of a heat conducting fluid in an asymmetric channel.

Therefore, the objective of the present paper is to investigate the effects of the phase shift and Hartmann number on the pumping characteristics of peristaltic flow in a two-dimensional asymmetric channel under the assumptions of long wavelength and low Reynolds number in a wave frame of reference with heat transfer.

2. Mathematical Formulation and Solution

We consider the peristaltic transport of a heat-conducting fluid in an asymmetric channel with flexible walls and asymmetry being generated by the propagation of waves on the channel walls traveling with same speed c but with different amplitudes and phases. We assume that a uniform magnetic field strength B_0 is applied in the transverse direction to the direction of the flow (i.e., along the direction of the y-axis) and the induced magnetic field is assumed to be negligible. Figure 3.1 shows the physical model of the asymmetric channel.

The channel walls are given by

$$Y = H_1(X, t) = a_1 + b_1 \cos\frac{2\pi}{\lambda}(X - ct), \qquad \text{(upper wall) (3.1a)}$$

$$Y = H_2(X, t) = -a_2 - b_2 \cos\left(\frac{2\pi}{\lambda}(X - ct) + \theta\right), \qquad \text{(lower wall) (3.1b)}$$

where b_1, b_2 are amplitudes of the waves, λ is the wavelength, $a_1 + a_2$ is the width of the channel, θ is the phase difference $(0 \le \theta \le \pi)$ and t is the time.

We introduce a wave frame of reference (x, y) moving with velocity c in which the motion becomes independent of time when the channel length is an integral multiple of the wavelength and the pressure difference at the ends of the channel is a constant (Shapiro et al. [8]). The transformation from the fixed frame of reference (X, Y) to the wave frame of reference (x, y) is given by $x = X - ct$, $y = Y$, $u = U - c$, $v = V$ and $p(x) = P(X, t)$, where (u, v) and (U, V) are the velocity components, p and P are pressures in the wave and fixed frames of reference, respectively.

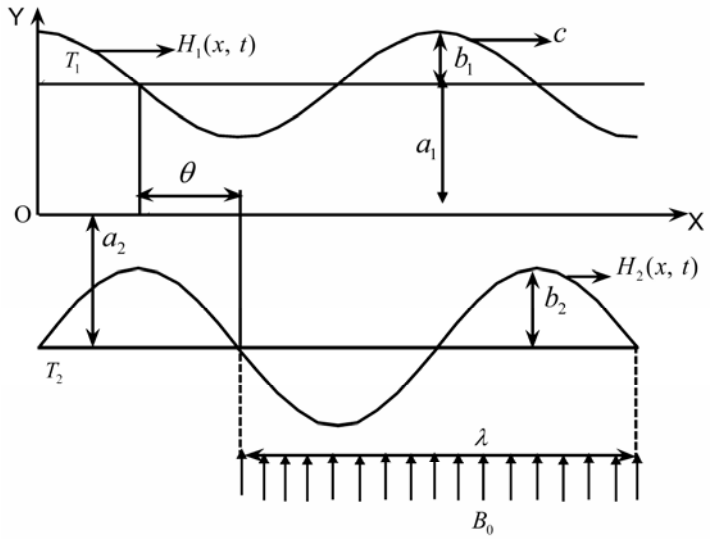

Figure 3.1. Physical model.

The equations governing the flow in wave frame of reference are given by

$$\frac{\partial u}{\partial x}+\frac{\partial v}{\partial y}=0, \tag{3.2}$$

$$u\frac{\partial u}{\partial x}+v\frac{\partial u}{\partial y}=-\frac{1}{\rho}\frac{\partial p}{\partial x}+\frac{\mu}{\rho}\left(\frac{\partial^2 u}{\partial x^2}+\frac{\partial^2 u}{\partial y^2}\right)-\frac{\sigma_e B_0^2}{\rho}u, \tag{3.3}$$

$$u\frac{\partial v}{\partial x}+v\frac{\partial v}{\partial y}=-\frac{1}{\rho}\frac{\partial p}{\partial y}+\frac{\mu}{\rho}\left(\frac{\partial^2 v}{\partial x^2}+\frac{\partial^2 v}{\partial y^2}\right), \tag{3.4}$$

and the equation of energy is

$$\rho c_p\left(u\frac{\partial T}{\partial x}+v\frac{\partial T}{\partial y}\right)=k\left(\frac{\partial^2 T}{\partial x^2}+\frac{\partial^2 T}{\partial y^2}\right)+2\mu\cdot\left[\left(\frac{\partial u}{\partial x}\right)^2+\left(\frac{\partial v}{\partial y}\right)^2\right]+\mu\left[\frac{\partial u}{\partial y}+\frac{\partial v}{\partial x}\right]^2, \tag{3.5}$$

where σ_e is the electrical conductivity of the fluid, ρ is the density, T is the temperature, c_p is the specific heat constant, k is the thermal conductivity and μ is the viscosity of the fluid.

Introducing the following non-dimensional variables

$$\bar{x}=\frac{x}{\lambda},\quad \bar{y}=\frac{y}{a_1},\quad \bar{u}=\frac{u}{c},\quad \bar{v}=\frac{v}{c\delta},\quad \delta=\frac{a_1}{\lambda},\quad d=\frac{a_2}{a_1},\quad \bar{T}=\frac{T-T_0}{T_2-T_0},$$

$$\bar{p}=\frac{pa_1^2}{\mu c\lambda},\quad h_1=\frac{H_1}{a_1},\quad h_2=\frac{H_2}{a_1},\quad \phi_1=\frac{b_1}{a_1},\quad \phi_2=\frac{b_2}{a_1},\quad T_R=\frac{T_1-T_0}{T_2-T_0},$$

where T_0 is the ambient temperature, in the governing equations (3.1)-(3.5), and dropping the bars, we get

$$h_1=1+\phi_1\cos 2\pi x,\quad h_2=-d-\phi_2\cos(2\pi x+\theta), \tag{3.6}$$

$$\frac{\partial u}{\partial x}+\frac{\partial v}{\partial y}=0, \tag{3.7}$$

$$Re\delta\left(u\frac{\partial u}{\partial x}+v\frac{\partial v}{\partial y}\right)=-\frac{\partial p}{\partial x}+\left(\delta^2\frac{\partial^2 u}{\partial x^2}+\frac{\partial^2 u}{\partial y^2}\right)-M^2 u, \tag{3.8}$$

$$Re\delta^3\left(u\frac{\partial v}{\partial x}+v\frac{\partial v}{\partial y}\right)=-\frac{\partial p}{\partial y}+\delta^2\left(\delta^2\frac{\partial^2 v}{\partial x^2}+\frac{\partial^2 v}{\partial y^2}\right), \tag{3.9}$$

and

$$\frac{Re\delta}{Ec}\left(u\frac{\partial T}{\partial x}+v\frac{\partial T}{\partial y}\right)$$

$$=\frac{1}{Ec\cdot Pr}\left(\delta^2\frac{\partial^2 T}{\partial x^2}+\frac{\partial^2 T}{\partial y^2}\right)+2\delta^2\left[\left(\frac{\partial u}{\partial x}\right)^2+\left(\frac{\partial v}{\partial y}\right)^2\right]+\left[\frac{\partial u}{\partial y}+\delta^2\frac{\partial v}{\partial x}\right]^2, \quad (3.10)$$

where $Re=\frac{\rho a_1 c}{\mu}$ is the Reynolds number, $M=B_0 a_1\sqrt{\frac{\sigma_e}{\mu}}$ is the Hartmann number, $Ec=\frac{c^2}{c_p(T_2-T_0)}$ is the Eckert number and $Pr=\frac{\mu c_p}{k}$ is the Prandtl number.

Using long wavelength (i.e., $\delta \ll 1$) and negligible inertia (i.e., $\mathrm{Re}\to 0$) approximations, we have

$$\frac{\partial p}{\partial y}=0, \quad \frac{\partial^2 u}{\partial y^2}-M^2u=P, \quad (3.11)$$

$$\frac{\partial^2 T}{\partial y^2}=Ec\cdot Pr\left(\frac{\partial u}{\partial y}\right)^2, \quad (3.12)$$

where $P=\frac{dp}{dx}$.

The corresponding non-dimensional boundary conditions are given as

$$u=-1 \quad \text{at} \quad y=h_1 \quad \text{and} \quad y=h_2, \quad (3.13)$$

$$T=T_R \quad \text{at} \quad y=h_1 \quad \text{and} \quad T=1 \quad \text{at} \quad y=h_2. \quad (3.14)$$

Solving equation (3.11) using the boundary conditions (3.13), we get

$$u=c_1\cosh My+c_2\sinh My-P/M^2, \quad (3.15)$$

where

$$c_1=\frac{(-1+P/M^2)[\sinh Mh_2-\sinh Mh_1]}{[\cosh Mh_1\sinh Mh_2-\cosh Mh_2\sinh Mh_1]}$$

and

$$c_2 = \frac{(-1 + P/M^2)[\cosh Mh_1 - \cosh Mh_2]}{[\cosh Mh_1 \sinh Mh_2 - \cosh Mh_2 \sinh Mh_1]}.$$

Solving equation (3.12) by using equation (3.15) and the boundary conditions (3.14), we get

$$T = -\frac{N}{8}(c_1^2 + c_2^2)\cosh 2My - \frac{Nc_1c_2}{4}\sinh 2My$$

$$- \frac{NM^2}{4}(c_2^2 - c_1^2)y^2 + c_3y + c_4, \tag{3.16}$$

where

$$c_3 = \frac{1}{(h_1 - h_2)}\left\{(T_R - 1) + \frac{N}{8}(c_1^2 + c_2^2)c_5 + \frac{Nc_1c_2}{4}c_6 + \frac{NM^2}{4}(c_2^2 - c_1^2)(h_1^2 + h_2^2)\right\},$$

$$c_4 = T_R + \frac{N}{8}(c_1^2 + c_2^2)\cosh 2Mh_1 + \frac{Nc_1c_2}{4}\sinh 2Mh_1 + \frac{NM^2}{4}(c_2^2 - c_1^2)h_1^2 - c_3h_1,$$

$$c_5 = (\cosh 2Mh_1 - \cosh 2Mh_2), \quad c_6 = (\sinh 2Mh_1 - \sinh 2Mh_2), \text{ and } N = Ec \cdot Pr.$$

The volume flow rate in the wave frame is given as

$$q = \int_{h_2}^{h_1} u\,dy$$

$$= \frac{c_1}{M}(\sinh Mh_1 - \sinh Mh_2) + \frac{c_2}{M}(\cosh Mh_1 - \cosh Mh_2) - \frac{P}{M^2}(h_1 - h_2). \tag{3.17}$$

From (3.12), we have

$$P = \frac{dp}{dx} = \frac{qM^3D_1 + D_2M^2}{D_2 - (h_1 - h_2)MD_1}, \tag{3.18}$$

where

$$D_1 = \cosh Mh_1 \sinh Mh_2 - \cosh Mh_2 \sinh Mh_1$$

and

$$D_2 = (\cosh Mh_1 - \cosh Mh_2)^2 - (\sinh Mh_1 - \sinh Mh_2)^2.$$

The instantaneous flux at any axial station is given by

$$Q(x, t) = \int_{h_2}^{h_1} (u + 1)\, dy = q + h_1 - h_2. \tag{3.19}$$

The average volume flow rate over one wave period $(T = \lambda/c)$ of the peristaltic wave is defined as

$$\overline{Q} = \frac{1}{T}\int_0^T Q dt = \frac{1}{T}\int_0^T (q + h_1 - h_2)\, dt = q + 1 + d. \tag{3.20}$$

The pressure rise over one wave length of the peristaltic wave is given by

$$\begin{aligned}\Delta p &= \int_0^1 \frac{dp}{dx}\, dx \\ &= \int_0^1 \frac{qM^3 D_1 + D_2 M^2}{D_2 - (h_1 - h_2) M D_1}\, dx \\ &= \int_0^1 \frac{(\overline{Q} - 1 - d) M^3 D_1 + D_2 M^2}{D_2 - (h_1 - h_2) M D_1} = \overline{Q} I_1 + I_2, \end{aligned} \tag{3.21}$$

where $I_1 = \int_0^1 \frac{M^3 D_1}{D_2 - (h_1 - h_2) M D_1}\, dx$ and $I_2 = \int_0^1 \frac{-(1 + d) M^3 D_1 + D_2 M^2}{D_2 - (h_1 - h_2) M D_1}\, dx.$

The equation (3.21) can be rewritten as

$$\overline{Q} = \frac{\Delta p - I_2}{I_1}. \tag{3.22}$$

3. Discussion of the Results

The variation of axial velocity u with y at $x = 0.25$ is calculated for different values of Hartmann number M and pressure gradient P with fixed $\phi_1 = 0.7$, $\phi_2 = 1.2$, $d = 2$, $\theta = 0$ in different cases (i) $P = -0.75$, (ii) $P = 0$ and (iii) $P = 0.75$ as depicted in Figure 3.2. The velocity profiles are parabolas. The maximum/minimum velocity occurs at the centre of the channel and increases as M increases. This is due to peristalsis. It is found that for positive values 'P', the reverse flow occurs when $M < 1$ and the opposite behaviour of the velocity is observed for $M > 1$.

Figure 3.3 shows the variation of axial velocity u with y for different values of Hartmann number M with $\phi_1 = 0.7,\ \phi_2 = 1.2,\ d = 2,\ \theta = \frac{\pi}{6}$ and for (i) $P = -0.75$, (ii) $P = 0$ and (iii) $P = 0.75$. For a given Hartmann number M, the maximum velocity decreases with the change in the values of pressure gradient P from negative to positive.

For a given pressure gradient P, the increase in the Hartmann number M, raises the velocity.

The variation of time averaged volume flow rate $\overline{Q}$ with pressure rise Δp for different phase shifts with $\phi_1 = 0.7,\ \phi_2 = 1.2,\ d = 2$ and for (i) $M = 0.5$ and (ii) $M = 1$ as shown in Figure 3.4. It is observed that in the pumping region and free pumping region as phase shift θ increases the time averaged flow rate as well as pressure rise both decrease. An interesting observation here is that in co-pumping region $\overline{Q}$ increases with phase shift θ for an appropriately chosen $\Delta p(< 0)$. Further, time averaged volume flow rate increases increase in the Hartmann number M.

Using equation (3.16), we have plotted the variation of temperature T with y for different values of Hartmann number M with $\phi_1 = 0.7,\ \phi_2 = 1.2,\ d = 2,\ \theta = 0,$ $T_R = 0.5,\ N = 2$ and for (i) $P = -0.75$, (ii) $P = 0$ and (iii) $P = 0.25$ and is shown in Figure 3.5. It is observed that the temperature T increases with the increasing y and attains the maximum value nearer to the lower wall of the asymmetric channel. Moreover, as Hartmann number M increases, the temperature will increase throughout the width of the channel. The similar behaviour is observed for $\theta = \pi/6$ is shown in Figure 3.6. Further, as phase shift θ increases, the temperature decreases.

The variation of temperature T with y for different values of Hartmann number M with $\phi_1 = 0.7,\ \phi_2 = 1.2,\ d = 2,\ \theta = 0,\ T_R = 1.5,\ N = 2$ and for (i) $P = -0.75$, (ii) $P = 0$ and (iii) $P = 0.25$ and is shown in Figure 3.7. The temperature profiles are parabolas for $M > 0.5$ when $P \geq 0$, the temperature profiles a straight line for $M = 0.5$. Figure 3.8 is drawn for variation of temperature with phase shift $\theta = \pi/6$. It is observed that the temperature shows the same behaviour as that of $\theta = 0$.

References

[1] H. L. Agrawal and B. Anwaruddin, Peristaltic flow of blood in a branch, Ranchi Univ. Math. J. 15 (1984), 111-121.

[2] A. A. Li, N. I. Nesteron, S. N. Malikova and V. A. Kilatkin, The use of an impulse magnetic field in the combined therapy of patients with stone fragments in the upper urinary tract, Vopr Kurortol Fizide. Lech Fiz Kult. 3 (1994), 22-24.

[3] Kh. S. Mekheimer, Peristaltic flow of blood under effect of a magnetic field in a non-uniform channels, Appl. Math. Comput. 153(3) (2004), 763-777.

[4] Kh. S. Mekheimer and T. H. Al-Arabi, Nonlinear peristaltic transport of MHD flow through a porous medium, Int. J. Math. Math. Sci. 26 (2003), 1663-1682.

[5] M. Mishra and A. Ramachandra Rao, Peristaltic transport of a Newtonian fluid in an asymmetric channel, Z. Angew. Math. Phys. 54 (2003), 532-550.

[6] A. H. Shapiro, M. Y. Jaffrin and S. L. Weinberg, Peristaltic pumping with long wavelengths at low Reynolds number, J. Fluid Mech. 37 (1969), 799-825.

[7] D. Tang and M. C. Shen, Peristaltic transport of a heat-conducting fluid subject to Newton's cooling law at the boundary, Internat. J. Engrg. Sci. 27 (1989), 809-825.

[8] D. Tang and M. C. Shen, Numerical and asymptotic solutions for the peristaltic transport of a heat-conducting fluid, Acta Mech. 83 (1990), 93-102.

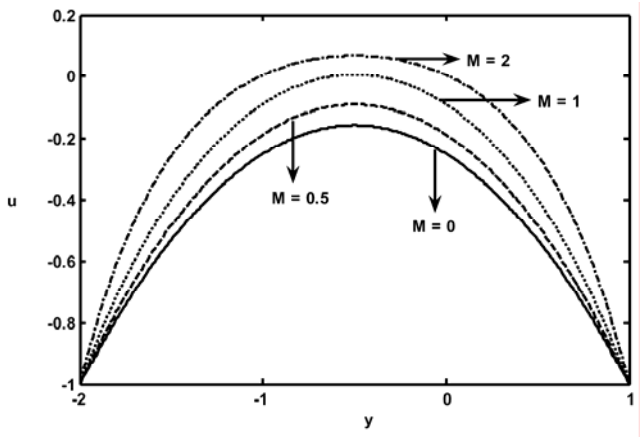

Figure 3.2 (i). The variation of velocity u with y for different values of M with $\phi_1 = 0.7$, $\phi_2 = 1.2$, $d = 2$, $\theta = 0$ and $x = 0.25$ for $P = -0.75$.

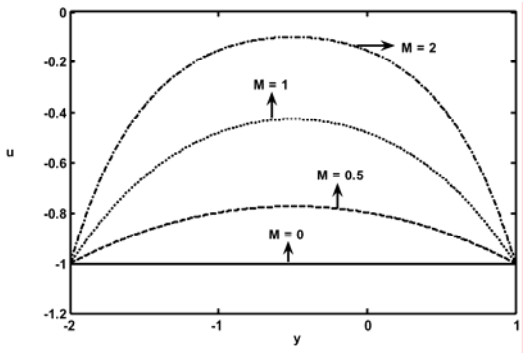

Figure 3.2 (ii). The variation of velocity u with y for different values of M with $\phi_1 = 0.7$, $\phi_2 = 1.2$, $d = 2$, $\theta = 0$ and $x = 0.25$ for $P = 0$.

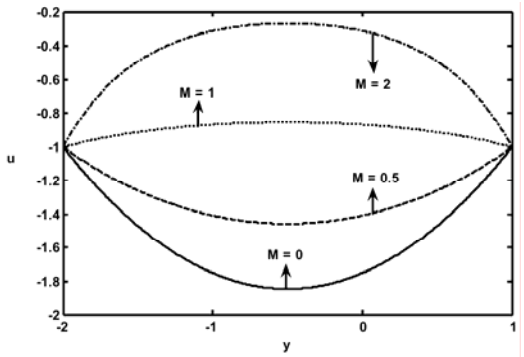

Figure 3.2 (iii). The variation of velocity u with y for different values of M with $\phi_1 = 0.7$, $\phi_2 = 1.2$, $d = 2$, $\theta = 0$ and $x = 0.25$ for $P = 0.75$.

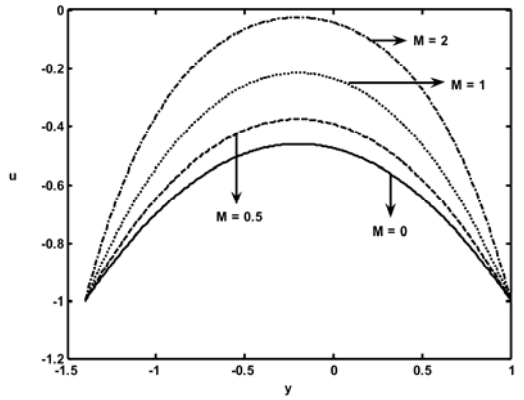

Figure 3.3 (i). The variation of velocity u with y for different values of M with $\phi_1 = 0.7$, $\phi_2 = 1.2$, $d = 2$, $x = 0.25$ and $\theta = \pi/6$ for $P = -0.75$.

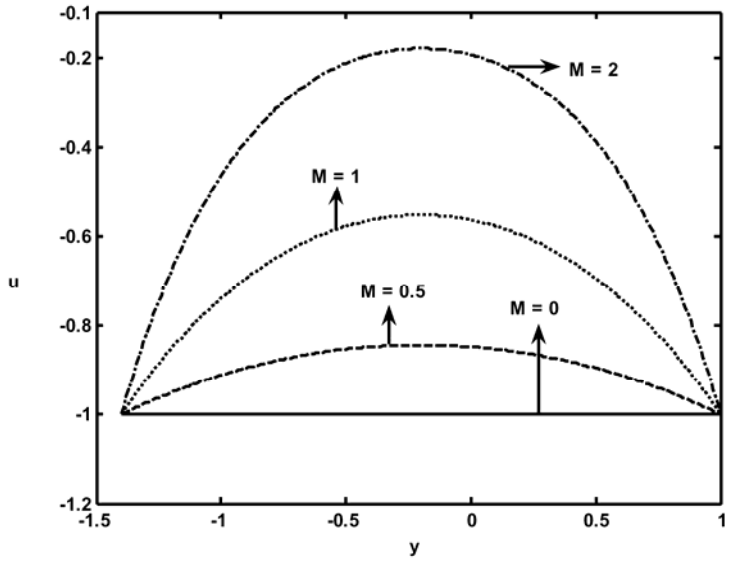

Figure 3.3 (ii). The variation of velocity u with y for different values of M with $\phi_1 = 0.7$, $\phi_2 = 1.2$, $d = 2$, $x = 0.25$ and $\theta = \pi/6$ for $P = 0$.

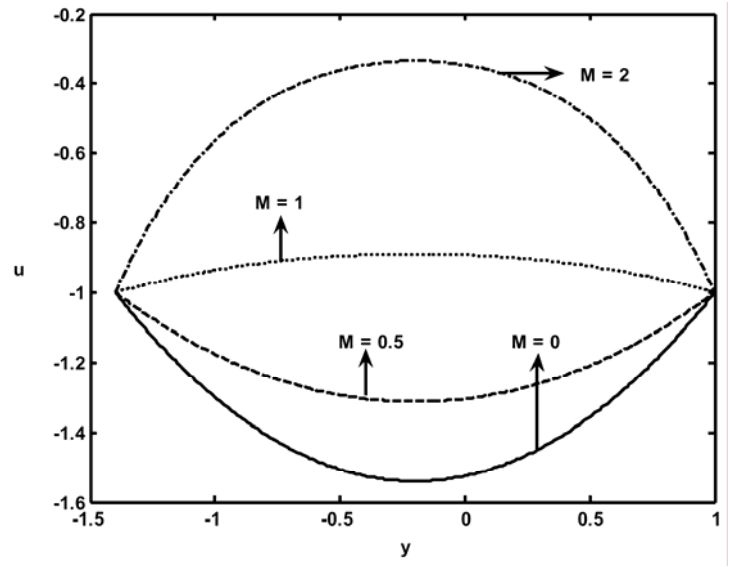

Figure 3.3 (iii). The variation of velocity u with y for different values of M with $\phi_1 = 0.7$, $\phi_2 = 1.2$, $d = 2$, $x = 0.25$ and $\theta = \pi/6$ for $P = 0.75$.

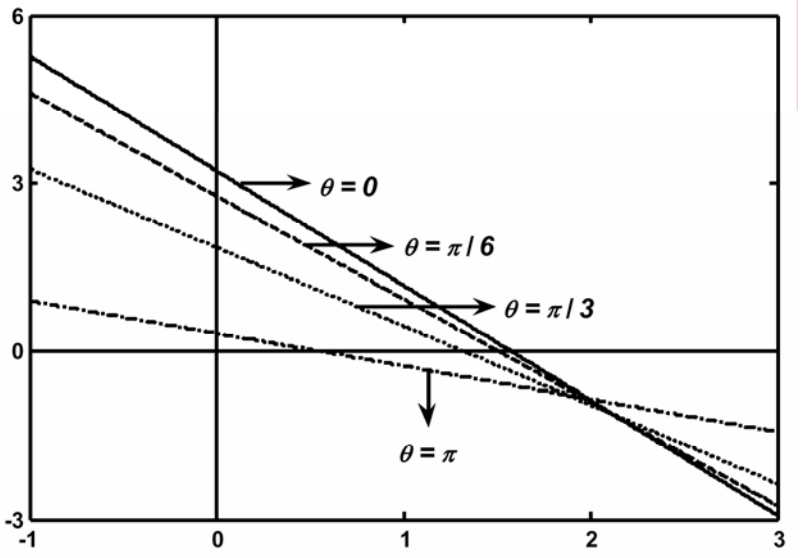

Figure 3.4 (i). The variation of pressure rise Δp with time-averaged volume flow rate $\overline{Q}$ for different phase shifts with $d = 2$, $\phi_1 = 0.7$, $\phi_2 = 1.2$ and $M = 0.5$.

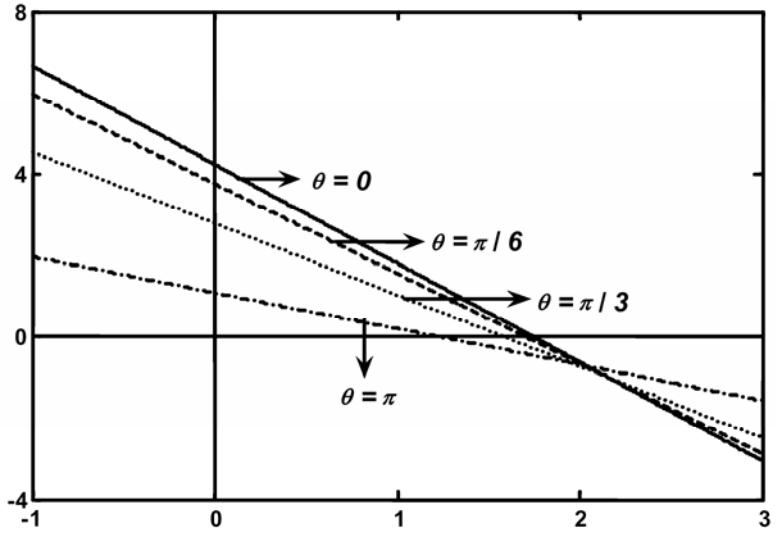

Figure 3.4 (ii). The variation of pressure rise Δp with time-averaged volume flow rate $\overline{Q}$ for different phase shifts with $d = 2$, $\phi_1 = 0.7$, $\phi_2 = 1.2$ and $M = 1$.

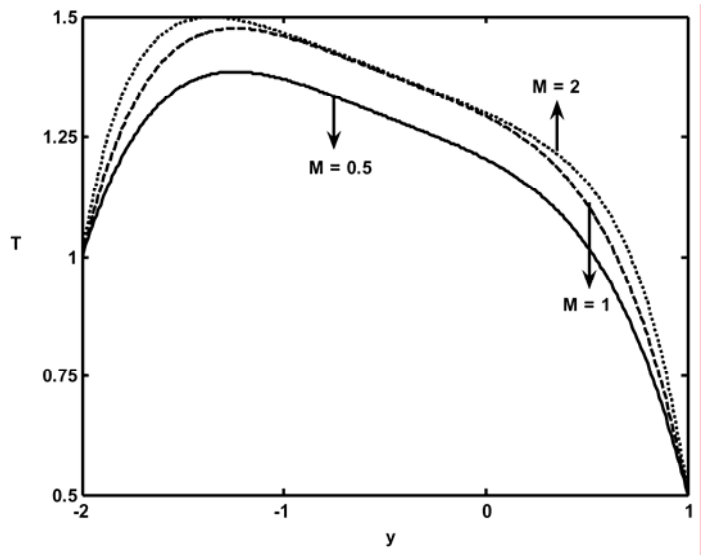

Figure 3.5 (i). The variation of temperature T with y for different values of Hartmann number M with $d = 2$, $\phi_1 = 0.7$, $\phi_2 = 1.2$, $x = 0.25$, $\theta = 0$, $T_R = 0.5$ and $N = 2$ for $P = -0.75$.

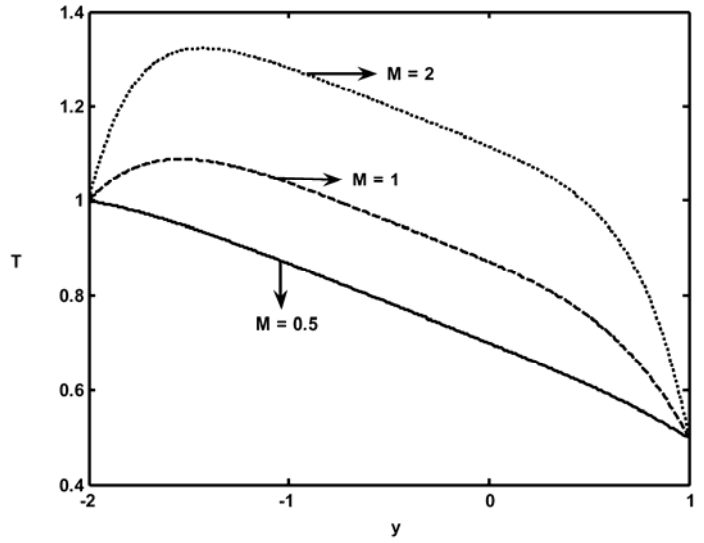

Figure 3.5 (ii). The variation of temperature T with y for different values of Hartmann number M with $d = 2$, $\phi_1 = 0.7$, $\phi_2 = 1.2$, $x = 0.25$, $\theta = 0$, $T_R = 0.5$ and $N = 2$ for $P = 0$.

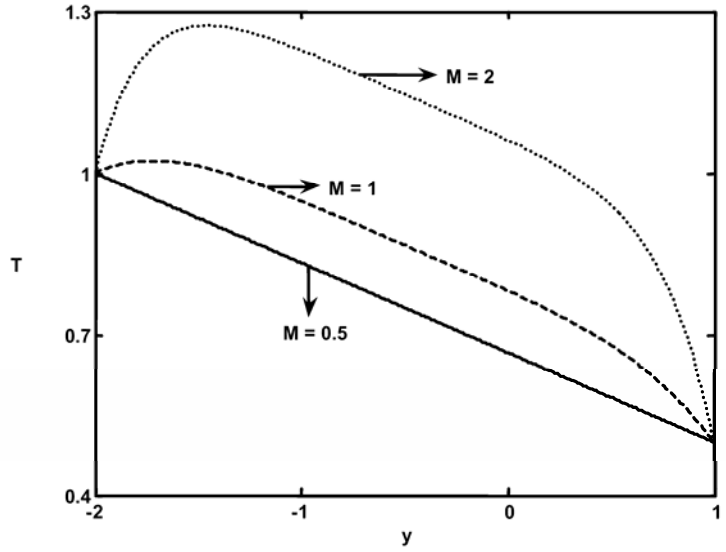

Figure 3.5 (iii). The variation of temperature T with y for different values of Hartmann number M with $d = 2$, $\phi_1 = 0.7$, $\phi_2 = 1.2$, $x = 0.25$, $\theta = 0$, $T_R = 0.5$ and $N = 2$ for $P = 0.25$.

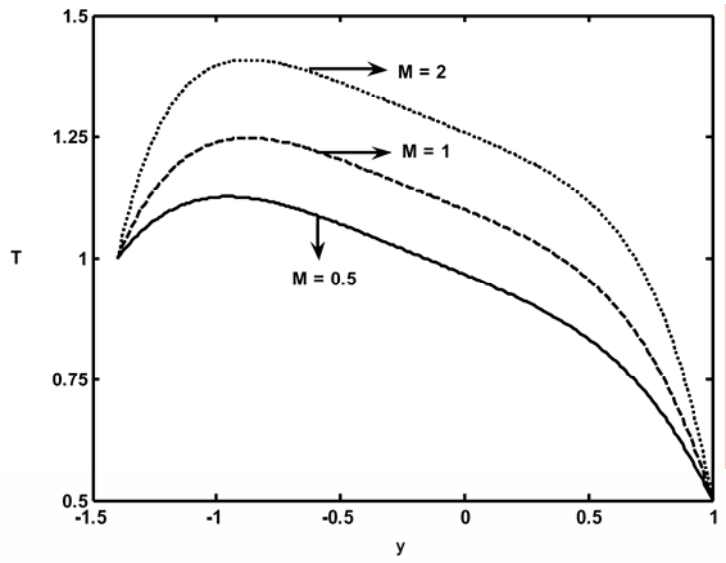

Figure 3.6 (i). The variation of temperature T with y for different values of Hartmann number M with $d = 2$, $\phi_1 = 0.7$, $\phi_2 = 1.2$, $x = 0.25$, $\theta = \pi/6$, $T_R = 0.5$ and $N = 2$ for $P = -0.75$.

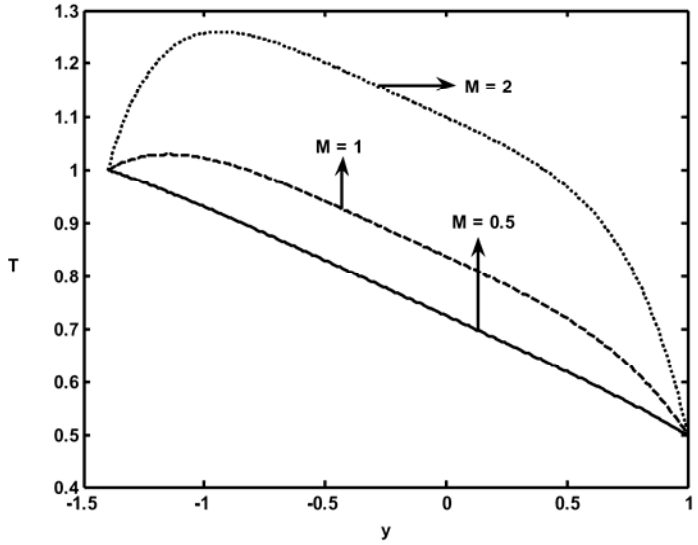

Figure 3.6 (ii). The variation of temperature T with y for different values of Hartmann number M with $d = 2,\ \phi_1 = 0.7,\ \phi_2 = 1.2,\ x = 0.25,\ \theta = \pi/6,\ T_R = 0.5$ and $N = 2$ for $P = 0$.

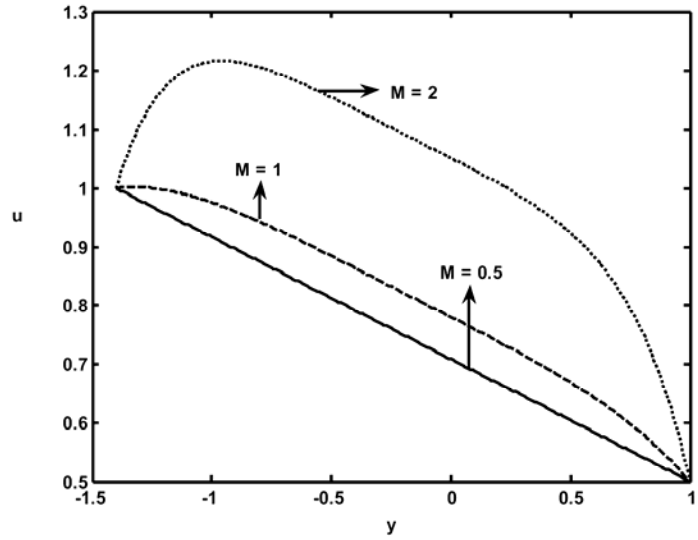

Figure 3.6 (iii). The variation of temperature T with y for different values of Hartmann number M with $d = 2,\ \phi_1 = 0.7,\ \phi_2 = 1.2,\ x = 0.25,\ \theta = \pi/6,\ T_R = 0.5$ and $N = 2$ for $P = 0.25$.

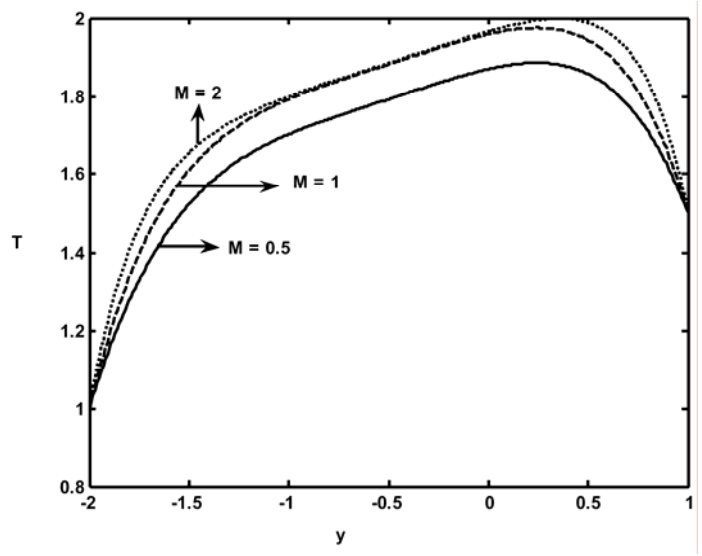

Figure 3.7 (i). The variation of temperature T with y for different values of Hartmann number M with $d = 2$, $\phi_1 = 0.7$, $\phi_2 = 1.2$, $x = 0.25$, $\theta = 0$, $T_R = 1.5$ and $N = 2$ for $P = -0.75$.

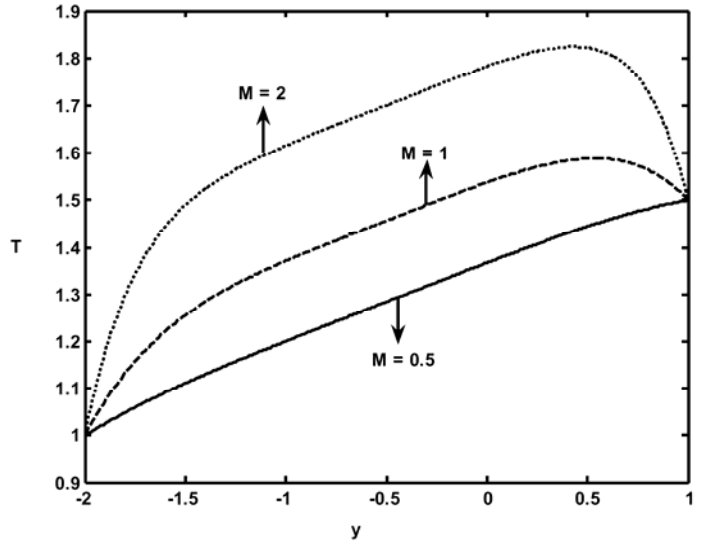

Figure 3.7 (ii). The variation of temperature T with y for different values of Hartmann number M with $d = 2$, $\phi_1 = 0.7$, $\phi_2 = 1.2$, $x = 0.25$, $\theta = 0$, $T_R = 1.5$ and $N = 2$ for $P = 0$.

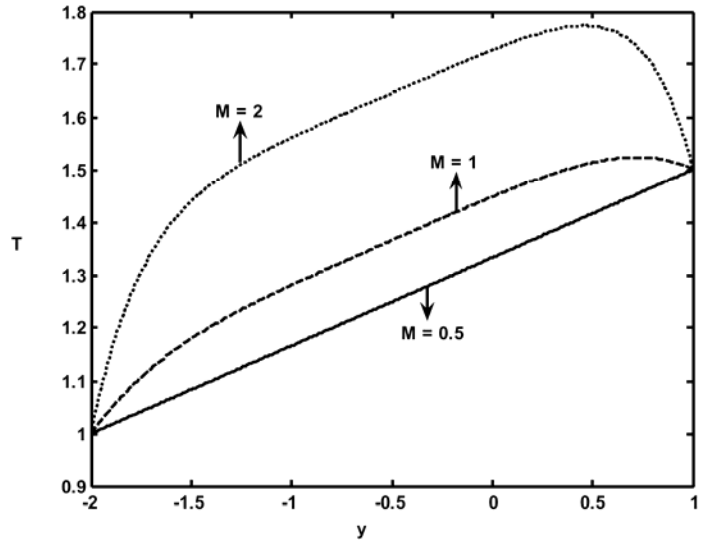

Figure 3.7 (iii). The variation of temperature T with y for different values of Hartmann number M with $d = 2$, $\phi_1 = 0.7$, $\phi_2 = 1.2$, $x = 0.25$, $\theta = 0$, $T_R = 1.5$ and $N = 2$ for $P = 0.25$.

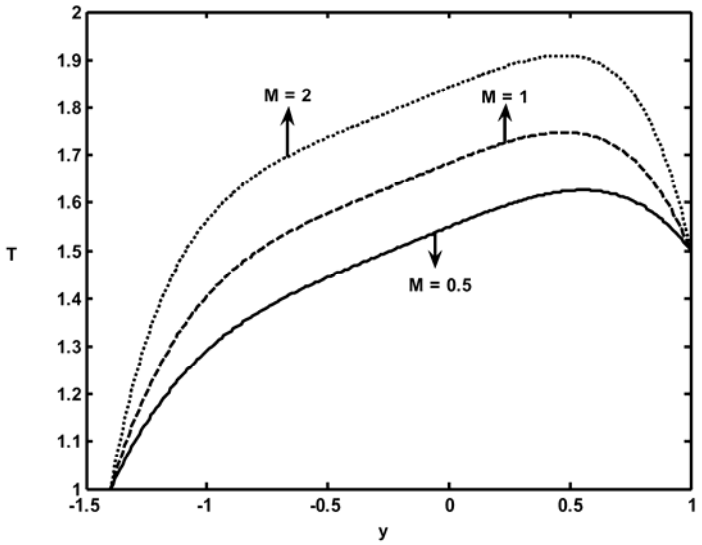

Figure 3.8 (i). The variation of temperature T with y for different values of Hartmann number M with $d = 2$, $\phi_1 = 0.7$, $\phi_2 = 1.2$, $x = 0.25$, $\theta = \pi/6$, $T_R = 1.5$ and $N = 2$ for $P = -0.75$.

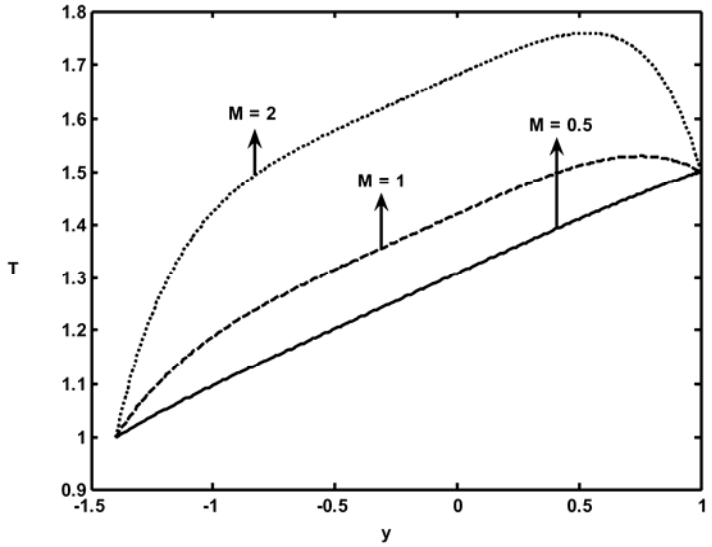

Figure 3.8 (ii). The variation of temperature T with y for different values of Hartmann number M with $d = 2$, $\phi_1 = 0.7$, $\phi_2 = 1.2$, $x = 0.25$, $\theta = \pi/6$, $T_R = 1.5$ and $N = 2$ for $P = 0$.

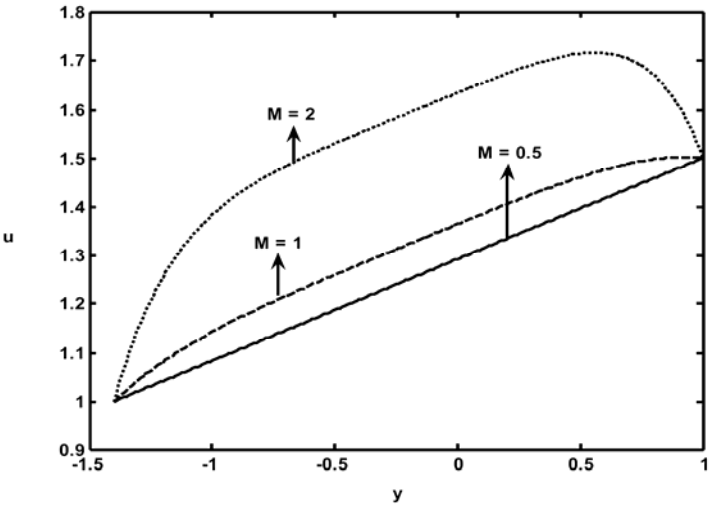

Figure 3.8 (iii). The variation of temperature T with y for different values of Hartmann number M with $d = 2$, $\phi_1 = 0.7$, $\phi_2 = 1.2$, $x = 0.25$, $\theta = \pi/6$, $T_R = 1.5$ and $N = 2$ for $P = 0.25$.